

RECENT ADVANCES IN MARINE SCIENCE
AND TECHNOLOGY, 92

NARENDRA K. SAXENA
EDITOR

PACON INTERNATIONAL
P.O. BOX 11568
HONOLULU, HAWAII 96828, U.S.A.

STORM SURGES AND TIDES AROUND SRI LANKA

R.F. Henry and T.S. Murty
Institute of Ocean Sciences
Sidney, British Columbia, Canada

ABSTRACT

On average, there has been about one damaging surge per decade in the waters around Sri Lanka, with more frequent smaller surges. Although the tidal range is not large, in surge forecasting it is important to have a detailed understanding of the tides, since damage is greater when peak surge coincides with high tide.

Study of storm surges and tides around Sri Lanka is made difficult by the shortage of meteorological and tide gauge records. There are a few relatively short coastal gauge records, but no deep sea tide gauges have been installed within several hundred kilometres of the Sri Lanka coast.

On the west coast of the island, there have been sudden increases in water levels forced by atmospheric gravity waves from mesoscale weather systems. Tropical cyclones from the south Andaman Sea normally pass north of Sri Lanka, but occasionally make landfall on the east coast, causing significant damage. The meteorological and surge information available from past events fall far short of requirements for full hindcasting studies.

Typical wind fields for cyclones, derived from observations in other tropical seas, were used to drive surge models for the east coast, and, similarly, typical wind fields for rissaga were assumed in studies of the west coast. Suitable conditions for forcing tidal models along their outer sea boundaries were deduced from cotidal charts computed with global tidal models, with some modification based on coastal gauge data.

INTRODUCTION

Storm surges are water level oscillations due to tangential surface wind stresses and sea level atmospheric pressure gradients associated with travelling weather systems. Tropical cyclone generated storm surges have had significant effects on the lands surrounding the Bay of Bengal and the Gulf of Mexico. Of the countries around the Bay of Bengal, Bangladesh experiences the most damaging surges, with India and Burma being somewhat less affected. It is not generally realized that Sri Lanka also has a storm surge problem, although the severity and frequency of storm surges there is much less than in Bangladesh.

In Sri Lanka, storm surges associated with tropical cyclones occur mostly on the northeast coast. Tropical cyclones are almost unknown on the west coast of Sri Lanka; however, flooding occurs on occasion, and the causes have never been satisfactorily accounted for. We suggest the so-called "Rissaga phenomenon" as one plausible explanation for the occasional high water levels on the west coast of Sri Lanka. Study of these meteorological effects on water levels is preceded by a discussion of tidal elevations, which, although rather small around Sri Lanka, cannot be ignored.

TIDES AROUND SRI LANKA

To our knowledge, there has been no publication to date in the open literature devoted to tides in the waters around Sri Lanka, although, some information is available from publications on tides in the Indian Ocean. Several studies on global ocean tides show co-tidal charts for the Indian Ocean (e.g., Schwiderski, 1980; Marchuk, et al., 1984). The resolution of the waters around Sri Lanka is so coarse in these models that it is almost impossible to obtain any detailed information on the tidal regime near the coasts.

The numerical model of Bogdanov and Kharkov (1976) for the Indian Ocean made use of a grid of $5^\circ \times 5^\circ$ in latitude and longitude; hence the co-tidal charts given for the two main semi-diurnal tidal constituents M_2 and S_2 and the two principal diurnal tidal constituents K_1 and O_1 do not contain much detail. By far the most detailed co-tidal charts produced for the north Indian Ocean are those of McCammon and Wunsch (1977). They constructed these charts by empirical methods from existing data and some deep ocean pressure gauge measurements. Even though these charts provided more detailed results than other studies, they are not detailed enough for the waters around Sri Lanka, except possibly near its southeast coast.

Henry and Murty (1983) and Elahi (1983) used numerical models to construct co-tidal charts for the Bay of Bengal and the Arabian Sea respectively. The modeled areas in these studies are essentially north of the study area and the results do not give any reliable information on tides around Sri Lanka. Thus it is fair to say that, until now, no detailed study of the tidal regime in the waters around Sri Lanka has been published. This paper is an initial effort to coordinate the limited information available.

THE NUMERICAL MODEL

The numerical model used here for simulating tides and storm surges covers a rectangular region from 7°N to 12°N and 77°E to 84°E (Figure 1). Figure 1 also shows the locations of the tide gauges from which data is used in this study. Contours of water depth are shown in Figure 2 and the grid for the numerical model is shown in Figure 3. The grid interval is 9 km in both horizontal directions.

In addition to the numerical simulation of selected storm surge events, our aim is to produce co-tidal charts for the largest constituents. For this purpose we start with the quasi-linear version of the shallow water equations.

$$\begin{aligned}\eta_t &= -(du)_x - (dv)_y \\ u_t &= -g\eta_x + fv - F^{(x)} + G^{(x)} \\ v_t &= -g\eta_y - fu - F^{(y)} + G^{(y)}\end{aligned}\tag{1}$$

where

- $\eta(x,y,t)$ = elevation of water surface above mean level
- $u(x,y,t)$ = depth-averaged velocity in x-direction
- $v(x,y,t)$ = depth-averaged velocity in y-direction
- $d(x,y)$ = mean water depth
- x,y = Cartesian coordinates in horizontal plane
- f = Coriolis coefficient (assumed constant)
- g = acceleration due to gravity
- t = time

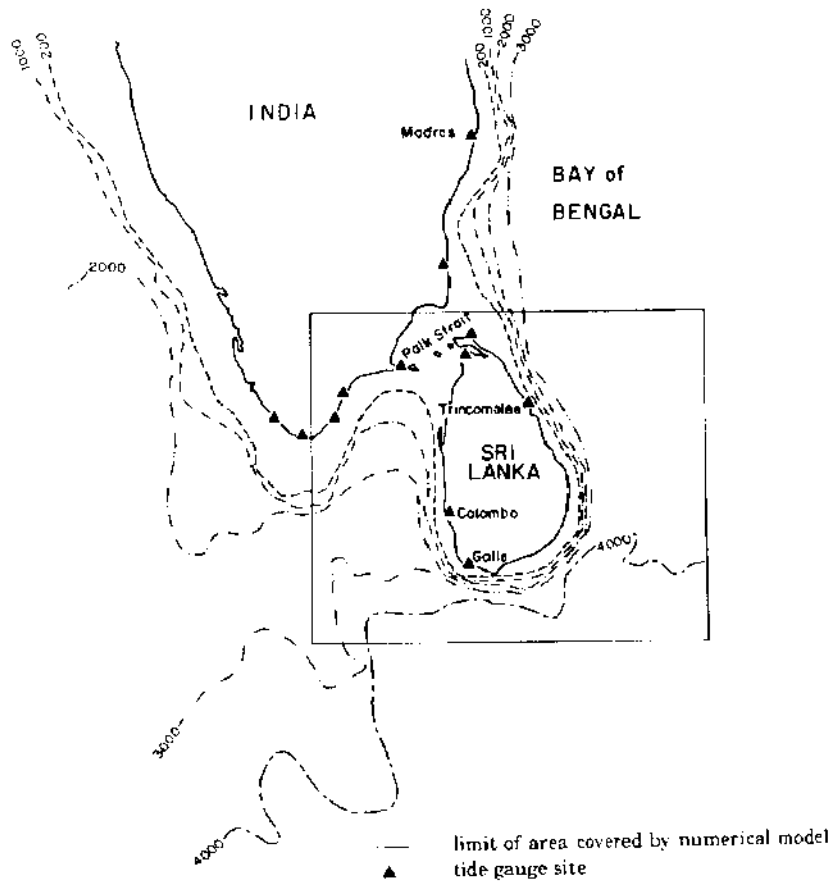


Figure 1. Study area (depths in metres)

$F^{(x)}$ and $F^{(y)}$ are the friction terms in the x and y directions respectively and are represented in the following way:

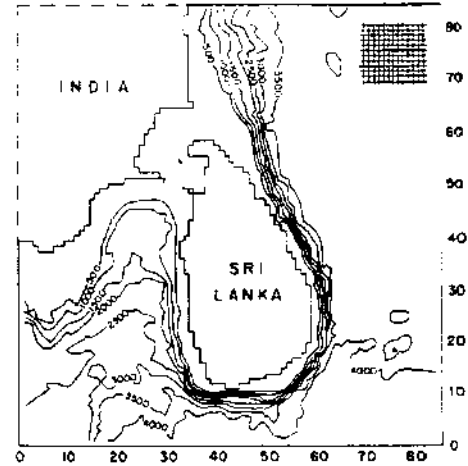
$$F^{(x)} = -\frac{ku(u^2 + v^2)^{1/2}}{d},$$

$$F^{(y)} = -\frac{kv(u^2 + v^2)^{1/2}}{d}.$$

where k is the coefficient of friction. A value of 2.5×10^{-3} was used for k . $G^{(x)}$ and $G^{(y)}$ are the forcing terms in the x and y directions respectively. In the tidal model the forcing

terms are put equal to zero, while in the storm surge model they represent the wind stress that drives the model.

Figure 2. Schematization of coastlines and contour plot of bathymetry used in model (depths in metres); portion of grid shown up upper right.



The following finite difference scheme is used as an approximation of the partial derivatives in the above equations (Figure 4):

$$\begin{aligned} \frac{\eta'_{ij} - \eta_{ij}}{\Delta t} &= \frac{(d_{ij} + d_{i+1,j})u_{i+1,j} - (d_{i-1,j} + d_{ij})u_{ij}}{2\Delta x} - \frac{(d_{ij} + d_{i,j+1})v_{i,j+1} - (d_{i,j-1} + d_{ij})v_{ij}}{2\Delta y} \\ \frac{u'_{ij} - u_{ij}}{\Delta t} &= -g \frac{\eta'_{ij} - \eta'_{i-1,j}}{\Delta x} + \bar{v}_{ij} - F_{ij}^{(x)} + G_{ij}^{(x)} \\ \frac{v'_{ij} - v_{ij}}{\Delta t} &= -g \frac{\eta'_{ij} - \eta'_{i,j-1}}{\Delta y} + \bar{u}_{ij} - F_{ij}^{(y)} + G_{ij}^{(y)} \end{aligned} \quad (2)$$

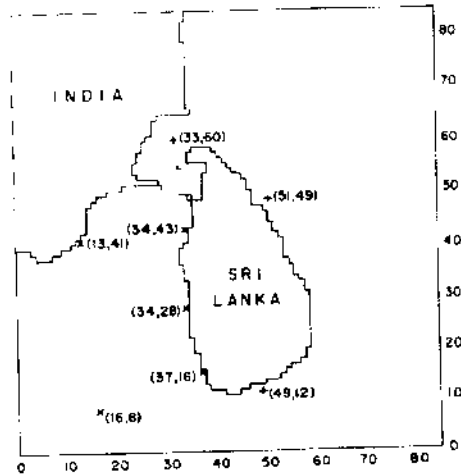
where

$$\begin{aligned} \Delta t &= \text{time step} \\ \Delta x, \Delta y &= \text{grid interval sizes in x,y directions respectively} \\ d_{ij} &= \text{mean water depth at elevation point } n_{ij} \\ \bar{u}_{ij} &= 1/4[u_{i,j-1} + u_{i+1,j-1} + u_{ij} + u_{i+1,j}] \\ \bar{v}_{ij} &= 1/4[v_{i-1,j} + v_{ij} + v_{i-1,j+1} + v_{i,j+1}] \end{aligned}$$

The primed values refer to terms updated during the current time step, while unprimed variables are the terms evaluated in the previous time step. The minimum time step permissible in order to maintain numerical stability is given by the following:

$$\Delta t \leq \frac{\Delta x \Delta y}{[gd_{\max}(\Delta x^2 + \Delta y^2)]^{1/2}} \quad (3)$$

where Δt is the time step, Δx and Δy are the grid mesh sizes in the corresponding directions, d_{\max} is the maximum depth of the model.



+ locations referred to in Figures 5 and 6
 x locations referred to in Figure 9

Figure 3(a). Model area showing specific elevation points

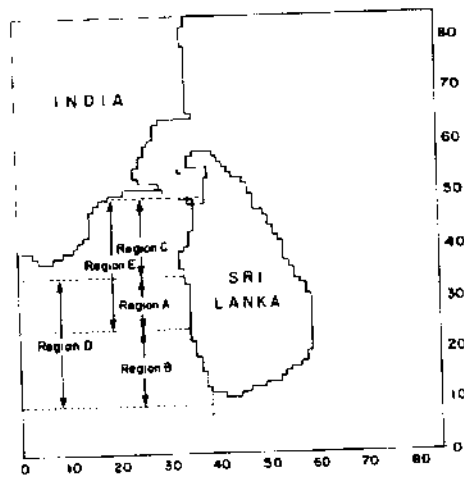


Figure 3(b). Model area showing wind forcing areas for simulated west coast surges

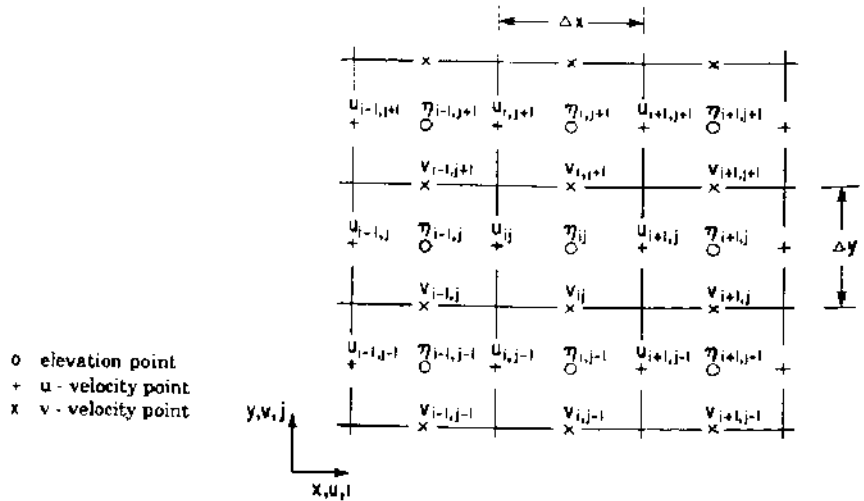


Figure 4. Richardson grid used in numerical model

The calculations carried out by the model depends on the location of the gridpoint. A land boundary, an open sea boundary and a point at the interior of the model all require different calculations. The model therefore allocates an integer code which describes the condition to be dealt with and which controls the corresponding calculation. If the boundary is closed (i.e., a coastline), it is assumed that there is no volume transport across the boundary. In other words, for a land boundary parallel to the y direction $u=0$; similarly if the land boundary is parallel to the x axis, then $v=0$. If the boundary is a sea boundary with a specified elevation, boundary conditions must be supplied. This situation is considered in the tidal model where boundary conditions are supplied by tide gauge harmonic analyses found from the Admiralty tide tables. A sea boundary with a radiating condition is considered in the storm surge model. This allows waves reaching the boundary of the model from within to radiate outwards.

For each boundary point an amplitude and a phase is prescribed as:

$$h(t) = A \cos(\omega t - \phi) \quad (4)$$

where $h(t)$ is the height of the wave at time t , A is the amplitude, ϕ is the phase at a given boundary point, ω is the frequency of the harmonic constituent being considered and t is the time. Values of A and ϕ at each open boundary point were obtained by judicious interpolation from existing large-scale cotidal charts, with some corrections from tide gauges on the Sri Lankan and Indian coasts.

The forcing terms for the storm surge model are supplied through the terms $G^{(x)}$ and $G^{(y)}$, given as:

$$G^{(x)} = -\frac{1}{\rho_a} \frac{\partial P_a}{\partial x} + \frac{\tau_{ux}}{\rho D} \quad \text{and} \quad G^{(y)} = -\frac{1}{\rho_a} \frac{\partial P_a}{\partial y} + \frac{\tau_{vy}}{\rho D} \quad (5)$$

where ρ is the density of water, ρ_a is the density of air, τ_{sx} , τ_{sy} are the components of wind stress in the x and y directions; $\frac{\partial P_a}{\partial x}$ and $\frac{\partial P_a}{\partial y}$ are the sea level atmospheric pressure gradients in the x and y directions (Murty, 1984).

Results from trial runs suggested that the contributions from the pressure gradient terms and the bottom stress terms were not significant, and hence these terms were omitted in certain runs. Then (5) becomes

$$G^{(x)} = \frac{\tau_{sx}}{\rho D} \quad \text{and} \quad G^{(y)} = \frac{\tau_{sy}}{\rho D} \quad (6)$$

The wind stress is given by

$$\tau_x = \rho_a K |V| V \quad (7)$$

where V is wind velocity and K is a drag coefficient. A value of 2.6×10^{-3} was used for K.

It can be seen from Figure 2 that the depth gradient is quite steep off the south-easterly coast of Sri Lanka. On the other hand, the gradient is quite small off the south coast of India. It is also to be noted that there are some shallow areas in Palk Strait. These features will have some effect on the results of the model runs.

To minimize model spin-up time, the amplitude of the tidal forcing was increased linearly over 15 hours of simulated time to the required magnitude, and the coefficient of friction k was set high initially and allowed to decrease exponentially to the required value.

Difference meteorological forcing is required for model studies of east and west coasts of Sri Lanka. Cyclones have been known to hit the East Coast of Sri Lanka. From Ali and Johns (1980), the wind velocity needed to determine $G^{(x)}$ and $G^{(y)}$ is given by:

$$\begin{aligned} V &= V_{\max} \left(\frac{r}{R} \right)^{3/2}, & 0 \leq r \leq R \\ V &= V_{\max} \left(\frac{R}{r} \right)^{1/2}, & r \leq R \end{aligned} \quad (8)$$

where r=radial distance from the centre of the cyclone and maximum wind speed V_{\max} occurs at radius R. A cyclone track and maximum wind speed were specified for each model run. On the west coast, surges were simulated by applying uniform wind fields over certain ocean areas. The wind was increased from zero to full strength over a period of two hours, held steady for two hours, and then gradually removed. Time series of surface elevation were recorded for prescribed points in the model domain during each run.

TIDAL MODEL RESULTS

Each tidal model run was monitored until steady oscillation was reached (eg., Figure 5(a),(b)) and harmonic analysis was then carried out. Avoiding abrupt application of the driving boundary conditions and artificially high initial damping, as described earlier, ensured that steady oscillation was reached within one or two cycles (see Figure 5(c),(d)). While tidal elevations always reached a steady oscillatory condition, velocities sometimes contained a low-frequency component (eg., Figure 6(g),(h)). This usually indicates the presence of topographically trapped waves created accidentally during the spin-up phase and not contributing to the elevation field. Since they are slow to dissipate and are well separated in frequency from the tidal constituent being studied, waves of this type can be ignored during the harmonic analysis.

Comparison of Figures 5(a) and (b) shows the marked effect of shallow waters on tidal behaviour. The tidal elevation record from point (33,60) in the shallows of Palk Strait shows attenuation of amplitude and presence of higher frequency harmonics.

An overall view of each tidal constituent can be shown most conveniently in the form of a cotidal chart. Figure 7(a) shows the computed amplitude for the largest tidal constituent, M_2 . Also shown are observed M_2 amplitudes at coastal tide gauges and the M_2 cotidal amplitudes as estimated by Vassie (personal communication, 1985). It can be seen that there is good agreement among all three. In general, the computed M_2 phase, shown in Figure 7(b), agrees well with the observed phase and also with Vassie's estimated co-phase pattern. Since most tide gauges are sited within harbours or estuaries, some differences between harbour readings and computed open coast

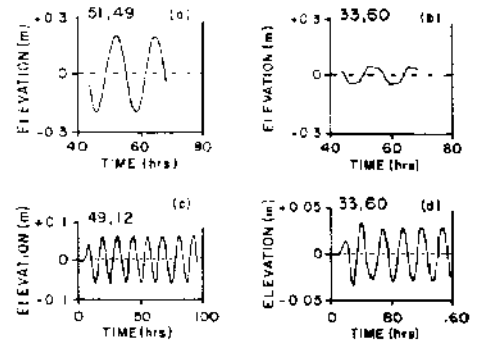


Figure 5. Computed tidal elevations
(a), (b) steady-state stage of M_2 simulation
(c) transient and steady-state stage of S_2 simulation
(d) transient and steady-state stage of O_1 simulation

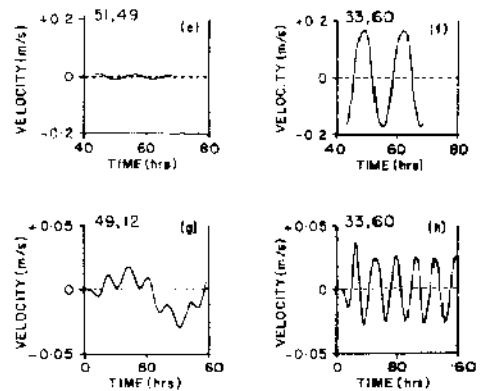


Figure 6. Computed tidal velocities (x-direction only)
(e), (f) steady-state stage of M_2 simulation
(g), (h) transient and steady-state stage of O_1 simulation

Better observations are available (Dharmaratha, 1985) for the next major surge in 1978, which is the one simulated here. The path of the cyclone as it crossed the east coast of Sri Lanka is shown in Figure 10(a). Also shown are three locations in the model grid where computer elevation was monitored. The wind distribution of Eq. (8) was used to represent the cyclone; this wind pattern was assumed to move along the cyclone track at 8 knots (14.8 kph). A maximum wind speed of 100 knots (185 kph) was adopted, in accordance with observed values. Though it is popularly assumed that the surge elevation is a maximum where a storm track crosses the coast, observations and the simulated surge shown in Figure 11 demonstrate that maximum elevations are experienced at coastal points, grid locations (3,57) and (16,16), somewhat beyond the region of maximum winds. The large surges at these two locations can be attributed partly to the shallow bathymetry in their neighbourhoods (Figures 10(b) and (c)). Where the cyclone path crosses the coast, point (20,33) in the model, the shelf is too narrow to amplify the surge, and in addition, the cyclone winds are parallel rather than normal to the coast.

WEST COAST STORM SURGE MODEL RESULTS

Even though there is no record of tropical cyclones ever impinging on the west coast of Sri Lanka, water level oscillations of significant amplitudes, up to 2.3 metres, have been observed on the coasts north and south of Colombo. The associated wave periods are of the order of 5-10 minutes, but unlike cyclone-generated surges, the whole event typically lasts 15-30 minutes. In fact, the meteorological events generating these water level oscillations are of even shorter duration. These episodes occur once or twice per year on average.

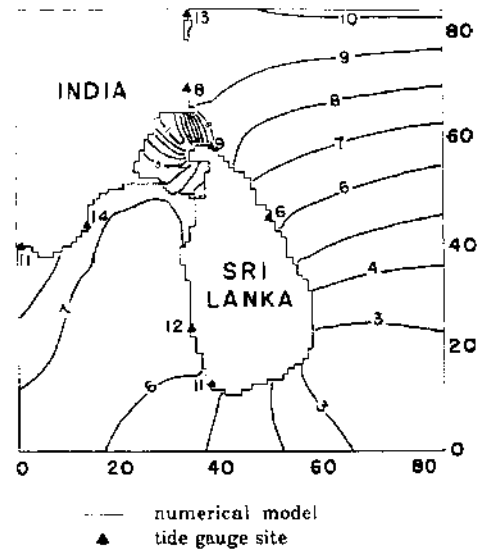


Figure 8(a). Co-amplitudes for S_2 constituent (cm)

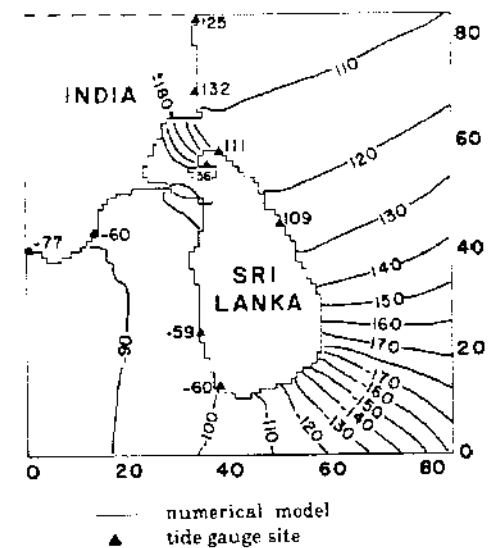


Figure 8(b). Co-phases for S_2 constituent (deg)

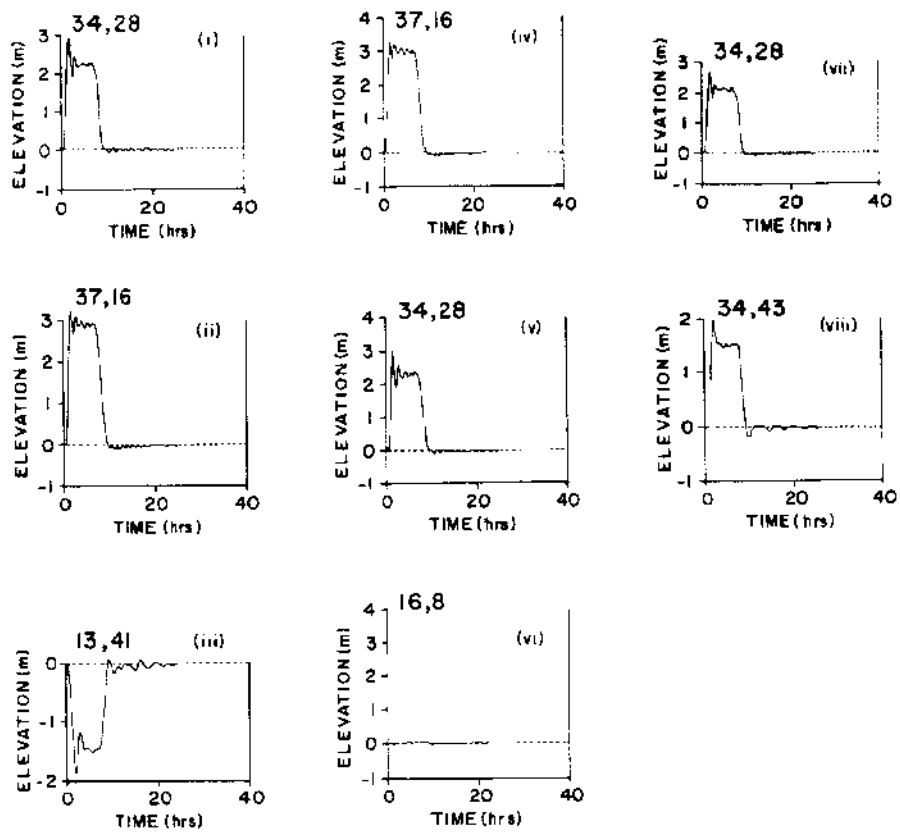


Figure 9. Simulated west coast storm surge elevations

- (i), (ii), (iii) Response to wind of 280 kph applied to regions A,B,C (Figure 3(b)) respectively
- (iv), (v), (vi) Response to wind of 280 kph applied to region D (vii) Response to wind of 280 kph applied to region E (viii) Response to wind of 150 kph applied to region E

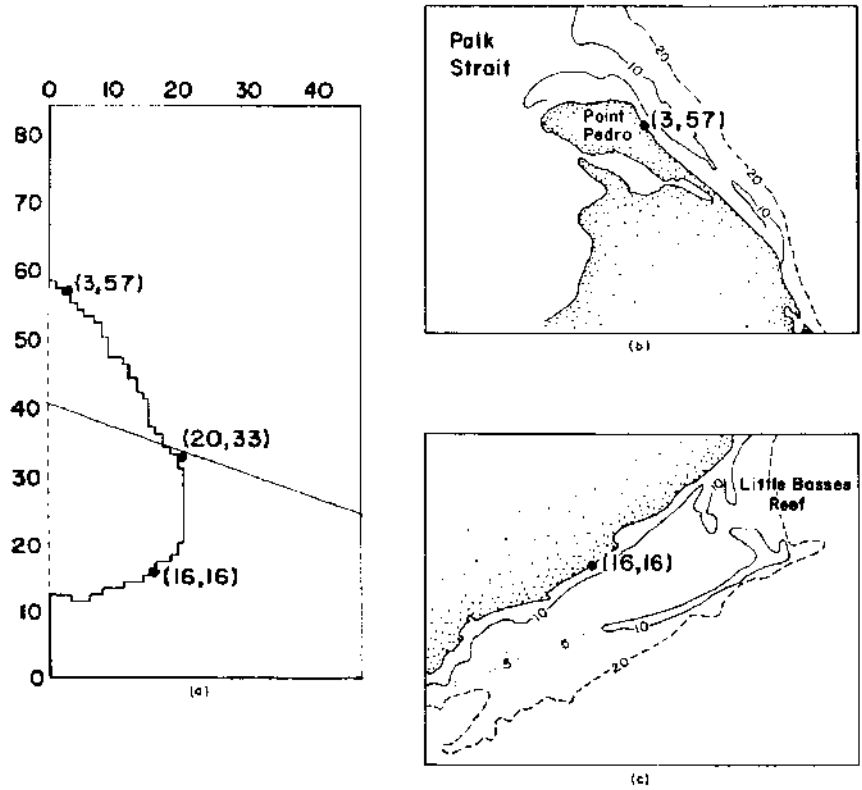


Figure 10. (a) Model grid details and track of simulated east coast cyclone
 (b), (c) Detail of bathymetry (depths in metres)

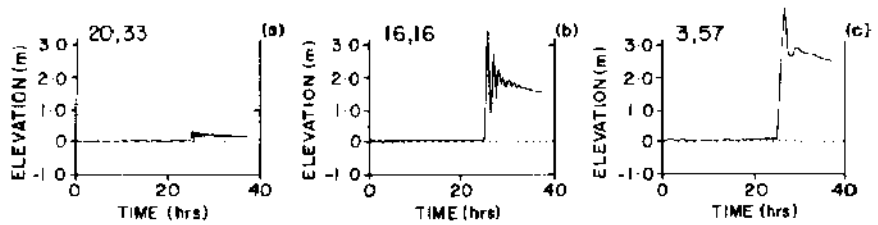


Figure 11. Computed elevations at 3 sites in Figure 10(a) during simulated east coast cyclone

Meteorological observations over the sea west of Sri Lanka are very sparse, but it seems likely that these brief surges are essentially similar to the "Rissaga phenomena" in the Mediterranean, discussed by Monserrat, et al. (1991). There, large short-term fluctuations in atmospheric pressure appear to cause corresponding fluctuations in water level, which are particularly noticeable wherever there is a resonant coupling between the atmospheric gravity wave and a normal mode of basin. In the Sri Lanka weather office records, there is evidence that strong wind gusts occur, extending some tens of kilometres along the coast and for an unknown distance seawards, while corresponding data on the pressure field is lacking. Consequently, in this study it was decided to examine the response in sea-level of the model to wind-fields corresponding in strength to reported cases and extending over different ocean regions west of Sri Lanka. The fact that similar effects were observed at the same time in Coochin, on the southwest coast of India, and north of Colombo suggests that the wind fields involved in these phenomena are quite extensive. The existence of normal shelf modes raises the possibility of some resonant amplification of water level at the coast, similar to that occurring in the Mediterranean.

Based on the sketchy data available, it was judged appropriate to use a wind directed at 10° south of east. Most cases were run at a wind speed of 280 kph, based on estimates of actual events. Significant water level oscillations are known to occur with wind-speeds down to 150 kph.

Model runs carried out with winds of the magnitude described above, applied to various regions, are shown in Figure 9. Whereas the computed maximum elevations are in the range of the reported amplitudes, the model needs over one hour to build up to these levels, which is slower than in nature. (The initial maximum water level is not affected by applying the wind field for longer than the initial phase, as was done in the model runs). There could be several reasons for this discrepancy. The actual phenomenon may have a lower, more quickly attained amplitude, but be subject to dynamic amplification to the observed levels. Physical factors which could cause such amplification are resonance with normal modes of vibration of the shelf and movement of the weather system.

The response is essentially similar in nature at different places on the Sri Lankan coast, though there is some variation with location and wind forcing region (Figure 9), whereas on the Indian coast (Figure 9(iii)), where the applied wind is offshore, the effect is inverted, as is to be expected. Far from the coasts, there is very little effect on sea-level (Figure 9(vi)).

CONCLUSIONS

To our knowledge, no publication has yet appeared on tides or storm surges in Sri Lankan waters. Although, in principle, much more sophisticated models could be developed, only a simplified model, without non-linear advection terms, has been used in this study. The sparsity of input data makes it pointless to use a more complicated model at this time. In future studies, including advection, all the tidal constituents would then be simulated together, to allow non-linear interaction be taken into account. In that case also, the surge modelling should be done simultaneously with the tidal simulation, as there can be interaction between the two.

ACKNOWLEDGMENT

We wish to thank Sylvia Harrison who did the computer programming for this study.

REFERENCES

- Johns, B., and A. Ali. 1981. Reply to J. Holland comment on paper by B. Johns and M.A. Ali, The numerical modelling of storm surges in the Bay of Bengal. *Quarterly Journal of the Royal Meteorological Society*. **107**(271-272).
- Anon. 1987. Admiralty Tide Tables. Hydrographer of the Navy, U.K.
- Bogdanov, K.T., and B.V. Kharkov, V. 1976. Calculation of Indian Ocean tides. *Oceanology*. **15**:156-150.
- Dharnaratha, C.H.P. 1985. Storm surge forecasting. Dept. Meteorology, Colombo 7.
- Elahi, K.Z. 1983. Tidal charts of the Arabian Sea north of 20°N. In: Proceedings of the U.N.E.S.C.O./R.O.P.M.E. Conference, ed. M.I. El-Sabh. Dhahran, Saudi Arabia. October.
- Gross, M.G. 1982. Oceanography: A View of the Earth. Third edition. New Jersey. pp 246.
- Henry, R.F. 1982. Automated programming of explicit shallow-water models with linearized models with linear or quadratic friction. *Canadian Technical Report of Hydrography and Ocean Sciences*. **3**.
- Marchuk, G.I., B.A. Kagan, and D.E. Cartwright (translation editor). 1984. Ocean Tides: Mathematical models and numerical experiments. Oxford: Pergamon Press. 176 pp.
- McCammon, C., and C. Wunsch. 1977. Tidal charts of the Indian Ocean north of 15°S. *Journal of Geophysical Research*. **82**(2037):5993-5998.
- Monserrat, S., A. Ibbetson, and A.J. Thorpe. 1991. Atmospheric gravity waves and the 'Rissaga' phenomenon. *Quarterly Journal of the Royal Meteorological Society*. **117**:553-570.
- Murty, T.S. 1984. Storm surges - meteorological ocean tides. Ottawa, Bulletin 212. *Canadian Journal of Fisheries and Aquatic Sciences*. pp 1-6, pp 41-44.
- Murty, T.S., and R.F. Henry. 1983. Tides in the Bay of Bengal. *Journal of Geophysical Research*. **88**(C10):6069-6076.
- Schwiderski, E.W. 1980. On charting global ocean tides. *Rev. Geophys. Space Phys.* **18**(1):243-268.